

Development 140, 1433-1444 (2013) doi:10.1242/dev.087551
© 2013. Published by The Company of Biologists Ltd

Single-cell gene expression profiling reveals functional heterogeneity of undifferentiated human epidermal cells

David W. M. Tan¹, Kim B. Jensen², Matthew W. B. Trotter³, John T. Connelly⁴, Simon Broad^{5,6} and Fiona M. Watt^{1,5,6,*}

SUMMARY

Human epidermal stem cells express high levels of $\beta 1$ integrins, delta-like 1 (DLL1) and the EGFR antagonist LRIG1. However, there is cell-to-cell variation in the relative abundance of *DLL1* and *LRIG1* mRNA transcripts. Single-cell global gene expression profiling showed that undifferentiated cells fell into two clusters delineated by expression of DLL1 and its binding partner syntenin. The DLL1⁺ cluster had elevated expression of genes associated with endocytosis, integrin-mediated adhesion and receptor tyrosine kinase signalling. Differentially expressed genes were not independently regulated, as overexpression of DLL1 alone or together with LRIG1 led to the upregulation of other genes in the DLL1⁺ cluster. Overexpression of DLL1 and LRIG1 resulted in enhanced extracellular matrix adhesion and increased caveolin-dependent EGFR endocytosis. Further characterisation of *CD46*, one of the genes upregulated in the DLL1⁺ cluster, revealed it to be a novel cell surface marker of human epidermal stem cells. Cells with high endogenous levels of CD46 expressed high levels of $\beta 1$ integrin and DLL1 and were highly adhesive and clonogenic. Knockdown of CD46 decreased proliferative potential and $\beta 1$ integrin-mediated adhesion. Thus, the previously unknown heterogeneity revealed by our studies results in differences in the interaction of undifferentiated basal keratinocytes with their environment.

KEY WORDS: Adhesion, CD46, Delta, Endocytosis

INTRODUCTION

Mammalian epidermis comprises a multi-layered epithelium [the interfollicular epidermis (IFE)] that forms the protective interface between the body and the environment, and associated adnexal structures. Whereas there are multiple stem cell populations in the hair follicle, maintenance of the IFE can be attributed to a single population of cells (Jaks et al., 2010). Long-term repair of burn injuries with cultured human IFE is a successful adult stem cell therapy and establishes unequivocally that IFE stem cells can be maintained and expanded in culture (Green, 2008).

Human IFE has a simple architecture. Stem cells reside in the basal layer of keratinocytes and terminal differentiation occurs in the suprabasal layers. Clonal growth is a functional marker of cultured human IFE stem cells (Barrandon and Green, 1987; De Luca et al., 2006) and has been used to identify cell surface markers. Markers that enrich for cells with high colony-forming ability include $\beta 1$ integrin extracellular matrix (ECM) receptors (Jones and Watt, 1993; Jones et al., 1995; Zhu et al., 1999), the Notch ligand

delta-like 1 (DLL1) (Lowell et al., 2000), the transmembrane proteoglycan MCSP (NG2, CSPG4) (Legg et al., 2003) and LRIG1 (Jensen and Watt, 2006), a transmembrane protein that negatively regulates the EGF receptor (EGFR) (Segatto et al., 2011).

Cells that express high levels of $\beta 1$ integrins, MCSP, LRIG1 and DLL1 lie in clusters in the IFE basal layer that have a specific location relative to the topography of the underlying basement membrane. Whole-mount labelling has revealed that cells within the clusters are less frequently proliferating than neighbouring cells and that the onset of differentiation occurs outside the clusters (Jensen et al., 1999).

Although immunolocalisation studies show that $\beta 1$ integrins, MCSP, LRIG1 and DLL1 are co-expressed in human epidermis, we previously observed that at the single-cell level this is not always the case (Jensen and Watt, 2006). In the present study we set out to examine by single-cell gene expression profiling whether the heterogeneous expression of individual stem cell markers is stochastic, reflecting transcriptional noise, or whether it reflects a previously unknown functional heterogeneity within the stem cell compartment (Chang et al., 2008; Kalmar et al., 2009; Oates, 2011).

MATERIALS AND METHODS

Cell culture

Work with human material was carried out in compliance with the UK Human Tissue Act (2004) and approved by the National Research Ethics Service (08/H0306/30). Primary human keratinocytes were isolated from neonatal foreskins of two individuals (strains kr and ky) and cultured on a feeder layer of J2-3T3 cells in FAD medium (one part Ham's F12, three parts Dulbecco's modified Eagle's medium, 1.8×10^{-4} M adenine), supplemented with 10% foetal calf serum (FCS) and a cocktail of 0.5 $\mu\text{g/ml}$ hydrocortisone, 5 $\mu\text{g/ml}$ insulin, 1×10^{-10} M cholera enterotoxin and 10 ng/ml epidermal growth factor (HICE cocktail) (Watt et al., 2006). Keratinocytes for siRNA transfection or culture on coverslips were grown in keratinocyte serum-free medium (KSFM, Gibco) supplemented with 30 $\mu\text{g/ml}$ bovine pituitary extract (BPE, Gibco) and 0.2 ng/ml recombinant EGF (rEGF, Gibco).

¹Epidermal Stem Cell Biology Laboratory, Wellcome Trust – Medical Research Council Cambridge Stem Cell Institute, Tennis Court Road, Cambridge, CB2 1QR, UK.

²Epithelial Development, Maintenance and Regeneration Laboratory, Wellcome Trust – Medical Research Council Cambridge Stem Cell Institute, Tennis Court Road, Cambridge, CB2 1QR, UK. ³Celgene Institute Translational Research Europe (CITRE), Parque Científico y Tecnológico 'Cartuja 93', Centro de Empresas Pabellón de Italia, Isaac Newton 4, Seville E-41092, Spain. ⁴Centre for Cutaneous Research, Barts and The London School of Medicine and Dentistry, 4 Newark Street, London, E1 2AT, UK. ⁵CRUK Cambridge Research Institute, Li Ka Shing Centre, Robinson Way, Cambridge, CB2 0RE, UK. ⁶Centre for Stem Cells and Regenerative Medicine, King's College London, 28th floor, Tower Wing, Guy's Campus, London, SE1 9RT, UK.

*Author for correspondence (fiona.watt@kcl.ac.uk)

This is an Open Access article distributed under the terms of the Creative Commons Attribution Non-Commercial Share Alike License (<http://creativecommons.org/licenses/by-nc-sa/3.0>), which permits unrestricted non-commercial use, distribution and reproduction in any medium provided that the original work is properly cited and all further distributions of the work or adaptation are subject to the same Creative Commons License terms.

Single-cell PCR

Keratinocytes (strain kr) used to generate cDNA libraries had been cultured for no more than three passages, were subconfluent, and had received fresh medium 24 hours before harvesting. Cells harvested in trypsin/EDTA were resuspended in complete FAD at 4°C and diluted in PBS. Single cells were collected by pipette and subjected to PCR essentially as described previously (Osawa et al., 2005; Jensen and Watt, 2006; Kurimoto et al., 2006).

To generate cDNA, a single cell or purified total RNA was placed in first-strand buffer (Superscript III buffer, Invitrogen), 0.5% Nonidet P40 (Pierce), 10 mM dNTP mixture (Roche), 3.4 nM MO₄dT₃₀ primer (5'-AAGCAGTGGTATCAACGCAGAGTGGCCATTACGGCCGTA CTTTTTTTTTTTTTTTTTTTTTTTTTTTTTTTTTTTTTTT-3') (Osawa et al., 2005), 1 mM DTT (Invitrogen), SuperRNaseIN (Ambion) and PrimeRNase inhibitor (Eppendorf), snap-frozen in liquid nitrogen and lysed at 65°C. Primer was allowed to anneal at 45°C before addition of Superscript III reverse transcriptase and incubation at 45°C. The reaction was inactivated at 65°C for 10 minutes. Unannealed primer was digested by exonuclease I (Thermo Fisher Scientific) with 6.7 mM MgCl₂ at 37°C. Removal of the RNA template and polyadenylation of the cDNA were carried out concurrently by the addition of RNaseH (Invitrogen), 1.5 mM dATP (Roche) and 30 units terminal deoxynucleotidyltransferase (TdT, Promega) at 37°C.

Four microlitres of polyadenylated cDNA was used as template for PCR amplification in 1× ExTaq buffer (TaKaRa), 0.65 mM dNTP (Roche), 8.25 μM MO₄dT₃₀ primer, 5 units ExTaq (TaKaRa) by incubating at 94°C for 1 minute, 50°C for 2 minutes, and 72°C for 2 minutes to allow second-strand synthesis. Subsequently, 35 cycles of amplification were performed by incubating at 94°C for 30 seconds, 60°C for 30 seconds, and 72°C for 2 minutes. The first round of amplification was performed in triplicate, after which the amplified cDNA was pooled. A second round of amplification was performed in duplicate as above using 2 μl of the pooled amplified cDNA as template. The amplified cDNA was again pooled before use.

Analysis of genes by PCR and QPCR

Screening single-cell cDNA libraries by PCR was carried out with ExTaq (TaKaRa) using 10 ng of the amplified samples. Quantitative (Q) PCR was performed using the SYBR Green detection system (Invitrogen) for all single-cell cDNA libraries or TaqMan probes (Applied Biosystems) for all other samples, as previously described (Frye et al., 2003). Real-time PCR was performed with an ABI Prism 7700 sequence detection system (Applied Biosystems). Relative quantification of each gene was determined using the standard curve method. The relative amount of each mRNA was normalised to the level of *B2M* or 18S ribosomal rRNA, as indicated. Primer sequences are provided in supplementary material Table S1.

cDNA labelling and Illumina BeadArray data analysis

cDNA was labelled essentially according to the manufacturer's instructions, except that the length of the *in vitro* transcription reaction was decreased to 6 hours. Labelled cDNA was hybridised to Illumina Human WG-6 v3 BeadArrays according to the manufacturer's instructions. Raw bead level data from these BeadArrays were imported and background corrected, via the beadarray package of the Bioconductor (<http://bioconductor.org>) suite of bioinformatics software, to the R statistical programming environment (<http://www.r-project.org>). Array probes that displayed significant hybridisation signal (Illumina signal detection statistic at $P < 0.01$; Bioconductor beadarray) in fewer than three of 18 profiles were removed prior to log₂ transformation and quantile normalisation (Bioconductor limma).

Interprofile similarity was assessed using hierarchical clustering with complete linkage and bounded interprofile dissimilarity of 1 – Pearson correlation. Two predominant profile clusters were identified and, for each array probe, differential expression between clusters was assessed using a moderated *t*-statistic (Bioconductor limma) with *P*-values corrected for the effects of multiple hypothesis testing over all probes using the false discovery rate (FDR) correction of Storey and Tibshirani (Storey and Tibshirani, 2003) (Bioconductor qvalue). Probes were deemed differentially regulated between profile clusters at an FDR threshold of 5% (*q*-value < 0.05) and subsequently annotated to genes using information provided by

the array manufacturer. Heat maps of gene expression were created by importing relevant subsets of processed microarray data into the Cluster 3.0 package (de Hoon et al., 2004).

IPA (Ingenuity Systems) was used to analyse the dataset of differentially expressed genes. The dataset containing gene identifiers and corresponding expression values was uploaded into the application. Each identifier was mapped to its corresponding object in the Ingenuity Knowledge Base and the biological functions that were most significant to the dataset were identified. Right-tailed Fisher's exact test was used to calculate a *P*-value for the probability that each biological function assigned to that dataset was due to chance alone.

Single-molecule RNA FISH

All reagents were prepared with nuclease-free water. Keratinocytes grown on glass coverslips were fixed in 3.7% paraformaldehyde (PFA) and permeabilised in 70% ethanol for at least 1 hour at 4°C. The catalogued Stellaris GAPDH-Quasar-570 RNA FISH probe set, as well as custom DLL1-Quasar-570 and LRIG1-FAM probe sets designed using the Stellaris Probe Designer, were purchased from Biosearch Technologies. Probe hybridisation was performed according to the manufacturer's instructions. In brief, *GAPDH* probe (125 nM) or *DLL1* and *LRIG1* probes (250 nM) were incubated with coverslips in hybridisation solution [10% dextran sulphate, 10% formamide in 2× saline-sodium citrate (SSC) buffer] at 37°C for at least 4 hours. Coverslips were washed twice by incubating with wash buffer (10% formamide in 2× SSC buffer) at 37°C for 30 minutes per wash, and mounted with ProLong Gold antifade reagent containing DAPI (Invitrogen). Cells were photographed using a Zeiss AxioImager microscope and images were submitted for blind 3D deconvolution (ten iterations) using Autodeblur (Media Cybernetics). Fluorescent dots were quantified using ImageJ software (NIH).

Retroviral infection

Retroviral vectors were packaged and keratinocytes were infected using virus-containing supernatant as previously described (Janes et al., 2004). The vectors used were: pBabePuro, pBabePuro-DeltaFl (Estrach et al., 2007) and pBabePuro-Lrig1Flag (gift from Yosef Yarden, Weizmann Institute, Rehovot, Israel) (Gur et al., 2004).

siRNA transfection

Cells were seeded in supplemented KSMF onto collagen I-coated plastic dishes the day before transfection. Transfection was performed with jetPRIME transfection reagent (Polyplus-Transfection, Nottingham, UK) and with 20 pmol per 10⁵ cells of ON-TARGETplus (Dharmacon, Lafayette, CO, USA) siRNAs J-003467 and J-010958 against *CAVI* and *CAV2*, respectively, siCD46 SMART-pool (L-004570) and siCD46-5 (L-004570-05) against *CD46*, and D-001810-10-05 non-targeting siRNA as a control. The medium was changed 24 hours after transfection and assays were performed after 72 hours.

Adhesion assays

Microtiter (96-well) tissue culture plates were coated with 50 μg/ml rat-tail type I collagen (BD Biosciences) in PBS before blocking with 1% heat-denatured BSA. Then, 20,000 cells were seeded into each well in quadruplicate in serum-free medium and incubated for 30 minutes at 37°C. After washing with PBS, cells were fixed with 4% PFA in PBS. Cells were stained with DiffQuik (International Reagents). Spread cells (defined as cells in which the long axis was more than twice the diameter of the nucleus) were counted in three independent fields per well.

Colony forming assays and IncuCyte analysis

Colony forming assays were performed by seeding 1000 keratinocytes per well of a 6-well plate on feeders in triplicate. Cells were cultured for 14 days, then fixed with 4% PFA and stained with 2% Rhodamine B and 2% Nile Blue (both Sigma-Aldrich). To obtain growth curves, cells were seeded in supplemented KSMF in triplicate wells of collagen I-coated 24-well Image-Lock plates (Essen Bioscience, Welwyn Garden City, UK). Data on cell numbers were collected on an IncuCyte live-cell imaging system (Essen Bioscience), where three independent fields per well were imaged at 1-hour intervals.

EGF stimulation assays

Keratinocytes cultured on J2-3T3 cells were grown to 80% confluence and then incubated overnight in FAD medium containing 0.5% serum. Cells were further serum-starved by incubation with unsupplemented FAD medium for 1 hour at 37°C. Then, 50 ng/ml EGF was added and cells were fixed at various time points with 4% PFA, then permeabilised and immunostained.

Immunofluorescence labelling

The following antibodies were used: zdd2 (1:100, anti-DeltaD, gift from J. Lewis, Cancer Research UK, London, UK), anti-FLAG M2 (1:1000, Sigma), anti-EGFR C-terminus (13G8, 1:1000, Millipore), anti-CAV1 (1:1000, Abcam), anti-CAV2 (1:200, Abcam), anti-CD46-PE (clone 8E2, eBioscience, Hatfield, UK) and anti-CD29 (ITGB1)-Alexa Fluor 647 (AbD Serotec, Oxford, UK). Cultured cells and frozen skin sections were fixed with 4% PFA for 20 minutes. In some experiments, cells were subsequently permeabilised with 0.1% Triton X-100 for 5 minutes at room temperature. Paraffin sections of surgical waste skin were de-waxed with xylene and subjected to antigen retrieval in citrate buffer (pH 6.0). Cells and sections were blocked for 1 hour at room temperature with 10% goat serum and 1% BSA or 0.25% fish skin gelatin in PBS. Primary antibody incubation was carried out for 1 hour at room temperature (cells) or overnight at 4°C (sections). Samples were labelled with Alexa Fluor (488 and 594)-

conjugated secondary antibodies for 1 hour at room temperature. Stained cells and sections were mounted in ProLong Gold antifade reagent containing DAPI and imaged using a Leica TCS SP5 confocal laser microscope or Zeiss AxioImager microscope.

Flow cytometry

Keratinocytes were labelled with fluorescently conjugated antibodies in blocking solution (1% BSA and 2 mM EDTA in PBS) for 30 minutes at 4°C and washed three times with blocking solution before flow sorting or analysis. To-Pro-3 was used to discriminate live and dead cells. Flow sorting was performed with a MoFlo cell sorter (Beckman Coulter, High Wycombe, UK) using 488 nm, 561 nm and 633 nm lasers.

RESULTS

Heterogeneous expression of stem cell markers

As illustrated in Fig. 1, we modified our previous protocol for generating single-cell cDNA libraries (Jensen and Watt, 2006) to improve their quality. We added an exonuclease I treatment step following first-strand synthesis to digest unannealed primer. This step was included because primer was added in excess during the first-strand synthesis step to ensure that all poly(A)-tailed RNA transcripts were reverse transcribed; polyadenylation of leftover

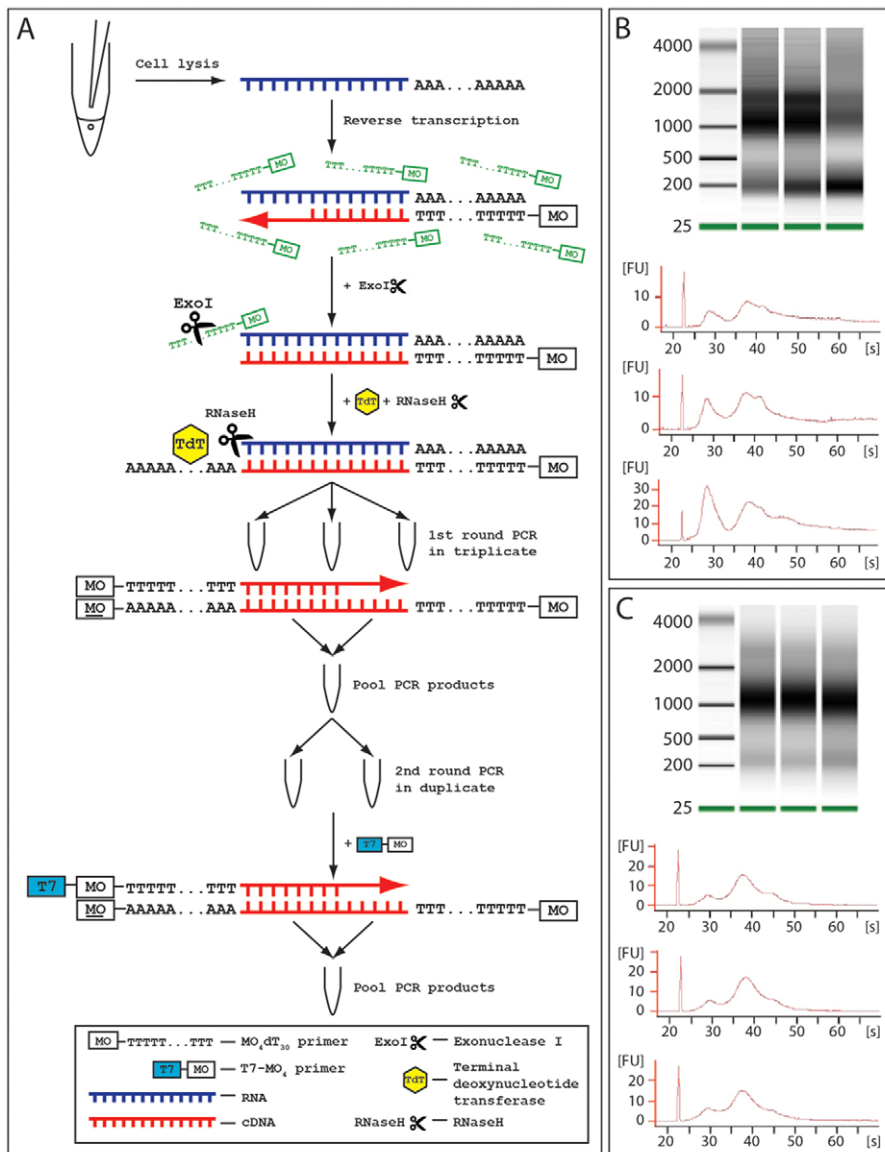


Fig. 1. Modification and optimisation of the single-cell PCR method. (A) Overview of the single-cell PCR method. (B,C) Electropherogram profiles of cRNA produced by an *in vitro* transcription (IVT) incubation of 16 (B) or 6 (C) hours. The standard 16-hour (overnight) IVT incubation produced samples that differed from the originals according to the bioanalyser traces (B). Our single-cell cDNA library method produces cDNA transcripts of only 500 to 1000 bp, which differs from standard reverse-transcribed total RNA samples that vary in transcript length. An IVT incubation of 6 hours (C) was optimal to obtain sufficient labelled cRNA with similar profiles to the original cDNA samples. The three samples are from individual single-cell cRNA libraries. The ladder shown is a RNA 6000 ladder (Agilent); the numbers indicate the size (in bases) of the RNA bands. FU, fluorescence units.

primer by the TdT enzyme would lead to concatemerisation and subsequent PCR amplification would lead to the build up of contaminating material (Kurimoto et al., 2006). Two replicate PCR amplifications were performed and the resulting PCR products were pooled to average out stochastic variation from the small sample size (Kurimoto et al., 2007). These modifications improved the efficiency of generating usable cDNA libraries from 30% to 92%.

The second PCR amplification step was modified with a primer that included a T7 promoter sequence for incorporation into the amplified cDNA to make it compatible with the standard Illumina *in vitro* transcription (IVT) protocol (Fig. 1A). The original protocol involved a more costly and labour-intensive labelling step that only incorporated one biotin-labelled nucleotide at the end of cRNA transcripts, compared with the Illumina IVT protocol that incorporates multiple biotin-labelled nucleotides.

We found that the standard 16-hour (overnight) IVT incubation produced samples that differed from the originals according to the bioanalyser electropherogram profiles (Fig. 1B). An IVT incubation period of 6 hours was optimal to obtain sufficient labelled cRNA with similar profiles to the original cDNA samples (Fig. 1C). A technical caveat of our method is that the reverse transcription reaction is kept short to ensure uniform amplification efficiency for all mRNA species (Kurimoto et al., 2007), such that only the last 500-700 bp at the 3' end of each transcript is amplified.

Abundance relationships were maintained between unamplified and amplified cDNA transcripts for *GAPDH*, *ACTB*, *B2M*, *ITGB1*, *K14* (*KRT14*) and *K10* (*KRT10*) (Fig. 2A). The detection of as few

as 40 copies of a spike RNA demonstrated the sensitivity of the method for amplifying low-abundance transcripts (Fig. 2B). Furthermore, there was good agreement between relative gene expression values of housekeeping genes (*ACTB* and *GAPDH*), markers of basal cells (*K14*, *ITGB1*) and differentiated cells (*K10* and *IVL*) measured by QPCR (Fig. 2C) and obtained from Illumina BeadArrays (Fig. 2D).

Single-cell cDNA libraries were produced from passage two and passage three primary human keratinocytes from a single donor (Fig. 3A). Live single-cell suspensions were examined under a dissecting microscope and picked on the basis of small size because keratinocytes enlarge as they undergo terminal differentiation. Each library was screened for expression of the housekeeping genes *GAPDH* and *B2M* and for two keratin genes: the IFE basal layer marker *K14* and the terminal differentiation marker *K10* (Fig. 3B).

Sixty-two single-cell cDNA libraries from undifferentiated keratinocytes ($K14^+$, $K10^-$) were examined for expression of *DLL1* and *LRIG1* (Fig. 3C). Only 21% of cells expressed both markers; the remaining cells expressed either one or neither. Eighteen libraries, chosen at random, were hybridised to Illumina BeadArrays. QPCR expression values of *DLL1* and *LRIG1* (Fig. 3D,E) were comparable with the microarray expression data (Fig. 3F,G).

To confirm cell-to-cell variation in *DLL1* and *LRIG1* expression, we visualised mRNA transcripts in keratinocytes using single-molecule RNA fluorescence *in situ* hybridisation (FISH) (Raj et al., 2008) (Fig. 3H-J). As a positive control, we detected *GAPDH* transcripts (Fig. 3H). Consistent with *GAPDH* being ubiquitously

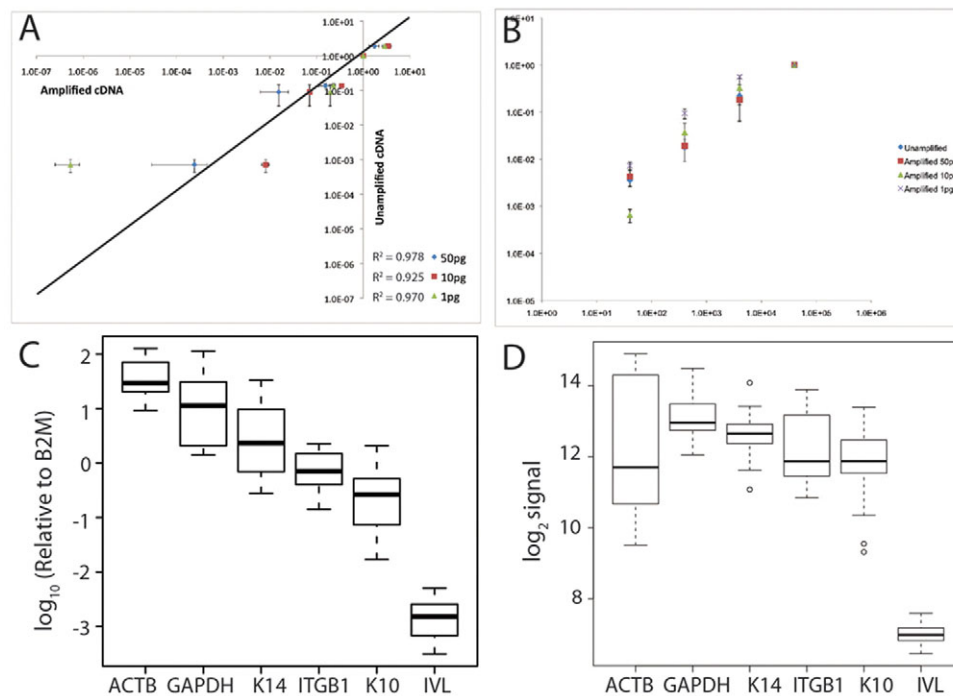


Fig. 2. Validation of the single-cell PCR method. (A) Expression values of cDNA generated from 100 ng total RNA plotted against expression values of cDNA generated and amplified from 50 pg, 10 pg and 1 pg total RNA. Correlation coefficient (R^2) values were 0.978, 0.925 and 0.970, respectively. Thus, linearity of relative transcript abundance was well preserved. (B) Addition of exogenous spike RNAs from *Arabidopsis thaliana* (*LTP4*, *LTP6*, *NAC1*, *TIM*) allows detection of transcripts of known copy number as an exogenous amplification control (Osawa et al., 2005). The spike RNA samples were diluted to known quantities and added to the first-strand synthesis buffer. Analysing the relative spike cDNA transcript levels after amplification showed that linearity was preserved in samples starting with 50 pg, 10 pg and 1 pg total RNA, where R^2 values were 0.994, 0.997 and 0.920, respectively. The spike RNA samples had been diluted to a concentration corresponding to ~40,000, 4000, 400 and 40 copies, respectively. Detection of 40 copies of a spike RNA demonstrates the sensitivity of the method for amplifying low-abundance transcripts. (C,D) Relative gene expression values of housekeeping genes (*ACTB* and *GAPDH*), markers of basal cells (*K14*, *ITGB1*) and differentiated cells (*K10* and *IVL*) as measured by QPCR (C) and obtained from Illumina BeadArrays (D). Data show mean \pm s.e.m.

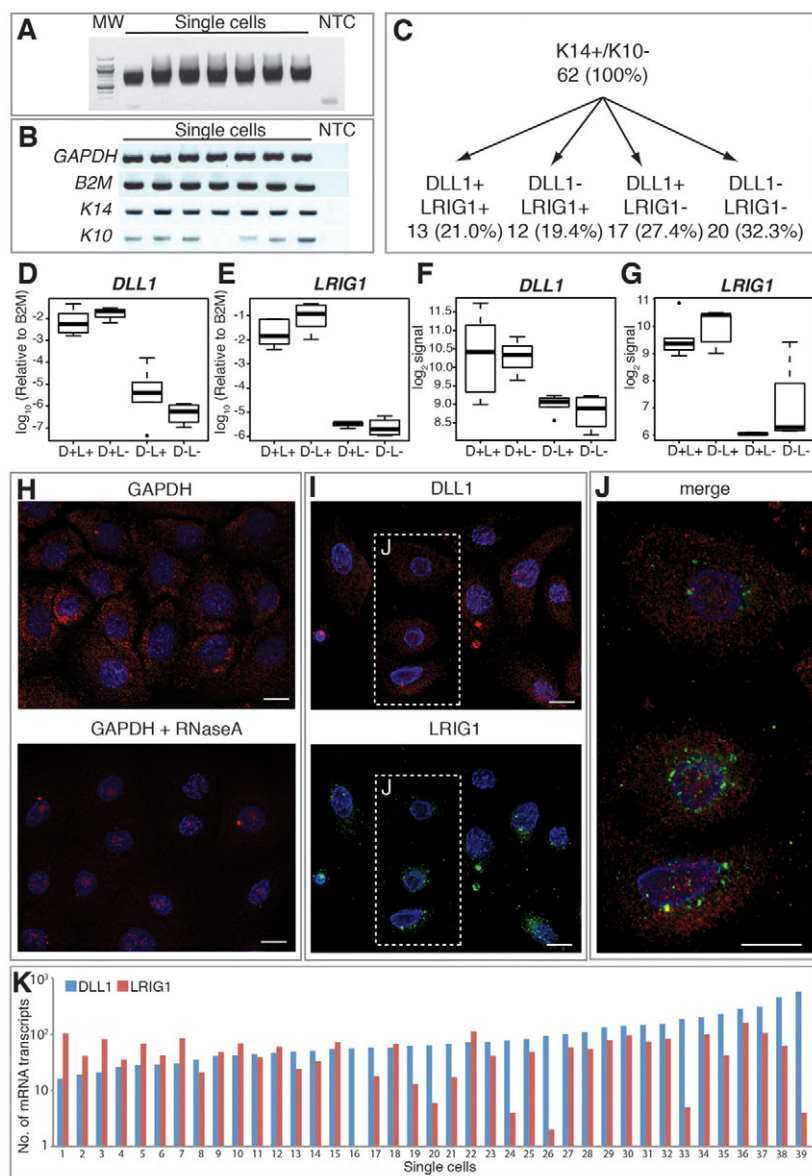


Fig. 3. Heterogeneous expression of stem cell markers at the single-cell level. (A) Seven single-cell cDNA libraries run on a 2% agarose gel show a smear of cDNA between 500 and 1000 bp. MW, molecular weight marker; NTC, no template control. (B) Marker expression in single-cell cDNA libraries determined by PCR. (C) Heterogeneous expression of *DLL1* and *LRIG1* in 62 single-cell cDNA libraries from keratinocytes that were *K14* positive and *K10* negative. (D,E) Relative gene expression values measured by QPCR for *DLL1* (D) and *LRIG1* (E). (F,G) Relative gene expression values obtained from Illumina BeadArrays for *DLL1* (F) and *LRIG1* (G). (H) Single-molecule RNA FISH with the *GAPDH* probe set. RNaseA treatment before probe hybridisation removes the cytoplasmic signal. (I) Simultaneous detection of *DLL1* and *LRIG1* mRNA by single-molecule RNA FISH shows cells with different levels of each type of transcript. (J) Merged image of boxed region in I at higher magnification. (K) Number of *DLL1* and *LRIG1* mRNA transcripts per cell in 39 single keratinocytes, ordered by level of *DLL1* expression. Data show mean \pm s.e.m. Scale bars: 20 μ m.

and highly expressed, numerous fluorescent dots were visible in the cytoplasm of all cells. The cytoplasmic signal disappeared when cells were treated with RNaseA before hybridisation (Fig. 3H). There was some nuclear signal in treated and untreated cells, which was judged to be nonspecific (Fig. 3H).

Single-labelled fluorescent probes were hybridised simultaneously to allow detection of *DLL1* and *LRIG1* transcripts in individual adherent (i.e. $\beta 1$ integrin⁺ undifferentiated) cells (Fig. 3I,J). The number of fluorescent dots in the cytoplasm of 39 single cells was quantified and ranked according to the number of *DLL1* dots (Fig. 3K). The results confirmed the observations from single-cell gene expression profiling (Fig. 3D-G) that the levels of *DLL1* and *LRIG1* were not obligatorily correlated at the single-cell level.

Single-cell global gene expression profiles cluster on the basis of *DLL1* expression

To examine the heterogeneity of individual undifferentiated human epidermal cells, global gene expression profiling of 18 individual cells was performed. Array data are deposited in ArrayExpress under Accession Number E-MTAB-824. An unsupervised approach

was adopted to assess interprofile similarity using hierarchical clustering. This revealed two predominant profile clusters (Fig. 4A) differing in *DLL1* expression, which we called the D⁺ and D⁻ clusters. All but one of the *DLL1*⁺ libraries clustered together, and although *LRIG1*⁺ cells were found in both clusters, all six *DLL1*⁺ *LRIG1*⁺ cells fell within the D⁺ cluster. In total, 2080 genes were significantly differentially expressed between the two clusters (Fig. 4A; supplementary material Table S2). The expression of a selection of differentially expressed genes was examined by QPCR of individual cells. In each case, the trends seen in the microarray expression data were confirmed (Fig. 4B). These data indicate that cells expressing the stem cell marker *DLL1*, including those that co-express a second stem cell marker, *LRIG1*, represent a discrete subpopulation of cells with similar transcriptional profiles that are distinct from other basal cells.

DLL1 marks cells that differ in adhesion and proliferation signalling

The dataset of 2080 differentially expressed genes was analysed using Ingenuity Pathway Analysis (IPA). Significant molecular and

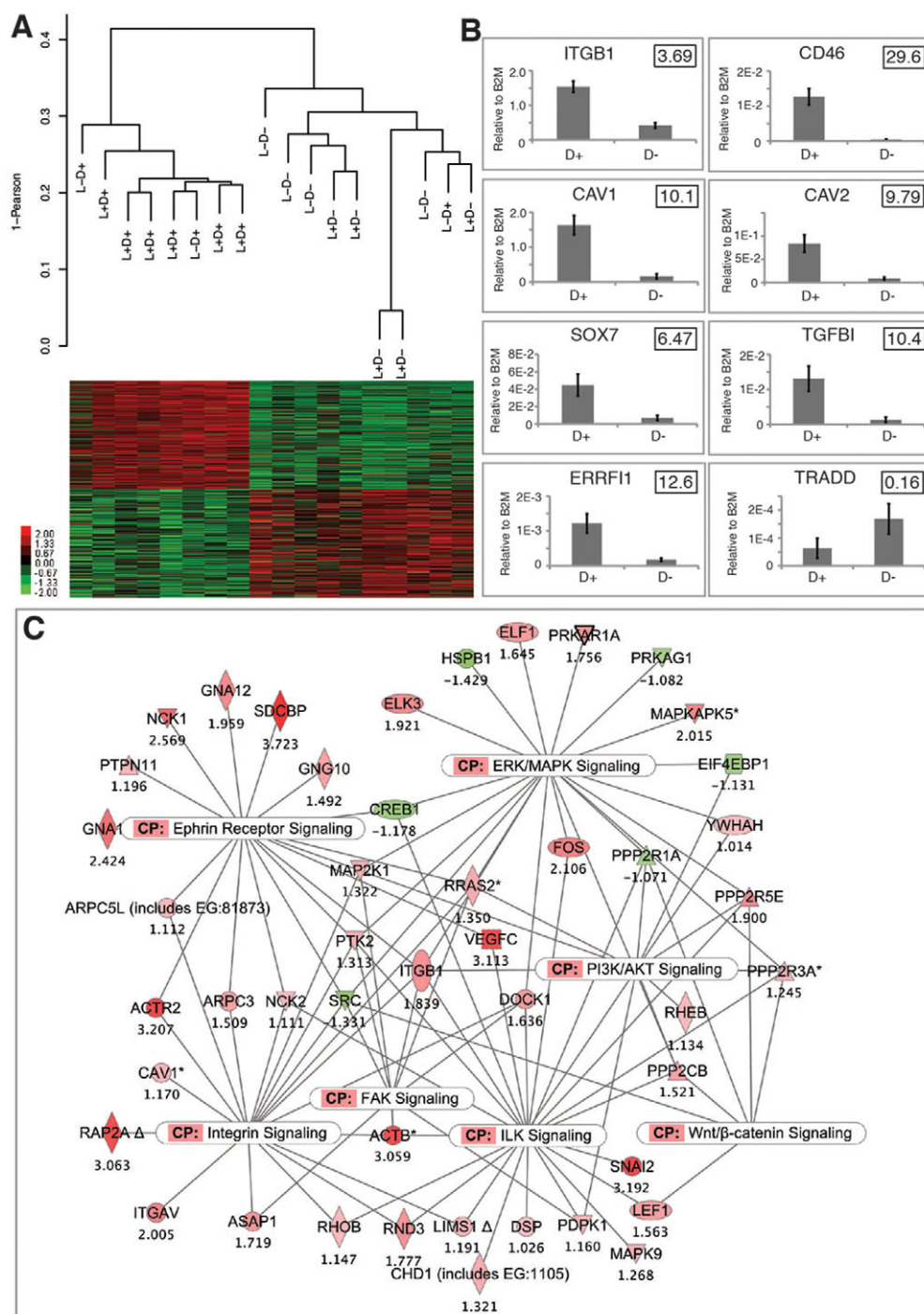


Fig. 4. Global gene expression profiling of single epidermal stem cells. (A) Unsupervised hierarchical clustering of 18 single-cell cDNA libraries and heatmap of differential gene expression of 2080 genes between the two clusters. D, *DLL1*; L, *LRI1*. **(B)** QPCR expression data for eight genes identified from the microarrays. Fold-change values obtained from Illumina BeadArrays are displayed in boxes in the upper right-hand corner. Data show mean \pm s.e.m. **(C)** IPA analysis showing canonical signalling pathway (CP) genes that were differentially expressed between the two clusters. Log₂ fold-change values (D+ cluster compared with D- cluster) are shown below coloured nodes.

cellular functions identified included gene expression, proliferation, cell cycle, cell death, and cytoskeletal organisation (supplementary material Table S3). Genes were mapped to canonical signalling pathways in the Ingenuity Knowledge Base (Fig. 4C). Major canonical pathways that differed between the D+ and D- libraries were adhesion related (integrin, ILK and FAK signalling) and proliferation related (ERK/MAPK, PI3K/AKT, ephrin receptor, Wnt/ β -catenin signalling) (Fig. 4C).

To find a better classifier of the two clusters than *DLL1*, we identified 150 genes with expression levels that were higher in every cell in one cluster than in every cell in the other cluster (supplementary material Table S4). IPA analysis revealed that the

top molecular and cellular functions and top canonical pathways were similar to those in the list of 2080 genes and included caveolin-mediated endocytosis (q -value= 5.45×10^{-3}) and integrin signalling ($q=1.60 \times 10^{-2}$). The gene that exhibited the greatest difference in expression between clusters was syntenin (upregulated $2^{3.723}=13.2$ -fold). We previously identified syntenin as a *DLL1*-binding protein that regulates *DLL1* endocytosis and *DLL1*-mediated cell adhesion (Estrach et al., 2007). Syntenin also interacts with the cytoplasmic domains of $\beta 1$ integrins and MCSF, two further stem cell markers (Beekman and Coffey, 2008). $\beta 1$ integrin was expressed in both clusters but was significantly upregulated ($2^{1.839}=3.6$ -fold) in the D+ cluster. Taken together,

these data indicate that DLL1 is a key discriminator of two types of human epidermal stem cell.

Overexpression of DLL1 and LRIG1 upregulates D+ cluster signature genes and increases cell adhesion and endocytosis

To test whether genes identified as upregulated in the D+ cluster were regulated independently of DLL1, we overexpressed DLL1 in keratinocytes by transduction with zebrafish *delta* (*deltaD*). We also examined the effect of overexpressing FLAG-tagged human *LRIG1*. Overexpression was confirmed by QPCR (Fig. 5A,B). Cells overexpressing *delta* were identified by labelling with a monoclonal antibody specific for zebrafish Delta (Lowell et al., 2000; Estrach et al., 2007) and *LRIG1*-overexpressing cells were detected with an antibody to the FLAG tag (Fig. 5C,D).

Cells overexpressing *delta* (D) alone or together with *LRIG1* (DL) showed significantly increased expression of D+ signature genes, including *ITGB1*, *CD46*, *CAV1*, *CAV2*, *TGFBI* and *SOX7* (Fig. 5E-J). Overexpression of *delta* alone caused a significant increase in all of these markers except *SOX7*. All six genes were significantly upregulated on combined overexpression of both stem cell markers. In the case of *ITGB1*, *CD46*, *CAV1* and *SOX7*, combined overexpression of *delta* and *LRIG1* resulted in a greater increase than overexpression of *delta* alone.

As predicted from the IPA analysis (Fig. 4C), *delta* and *LRIG1* overexpression increased ECM adhesion. DL cells were significantly more spread than control cells (transduced with empty vector) when plated on type I collagen (Fig. 5K). There was a small,

but not statistically significant, increase in spreading in D cells (Lowell and Watt, 2001).

One of the other top canonical pathways identified by IPA analysis in the D+ cluster was caveolin-mediated endocytosis signalling. DLL1 endocytosis and recycling are known to enhance DLL1 signalling activity (Wang and Struhl, 2004; Le Borgne, 2006; Nichols et al., 2007), and in keratinocytes DLL1 is readily detected in the endocytic compartment (Lowell et al., 2000; Estrach et al., 2007). To examine whether *delta* overexpression affected caveolin-mediated endocytosis, cells were serum starved and then stimulated with EGF. DLL1 overexpression did not alter total EGFR levels, nor the kinetics of stimulation of EGFR phosphorylation (data not shown). By analysing EGFR endocytosis at intervals (0, 5, 15, 30 and 60 minutes) in control cells, we determined that it took at least 15 minutes for the majority of cell surface EGFR to enter the endocytic compartment (data not shown). When quantitated at 20 minutes, there was a significant increase in the number of caveolin-positive endocytic vesicles in D and DL cells compared with controls (Fig. 5L,M). These results suggest that a functional consequence of the upregulation of *CAV1* and *CAV2* upon overexpression of *delta* is the increased endocytosis of cell surface growth factor receptors such as the EGFR.

We conclude that genes identified in the D+ cluster are not independently regulated because overexpression of Delta alone or in combination with LRIG1 can lead to increased expression of D+ genes. In addition, expression of D+ signature genes affects the interaction of undifferentiated keratinocytes with their external environment.

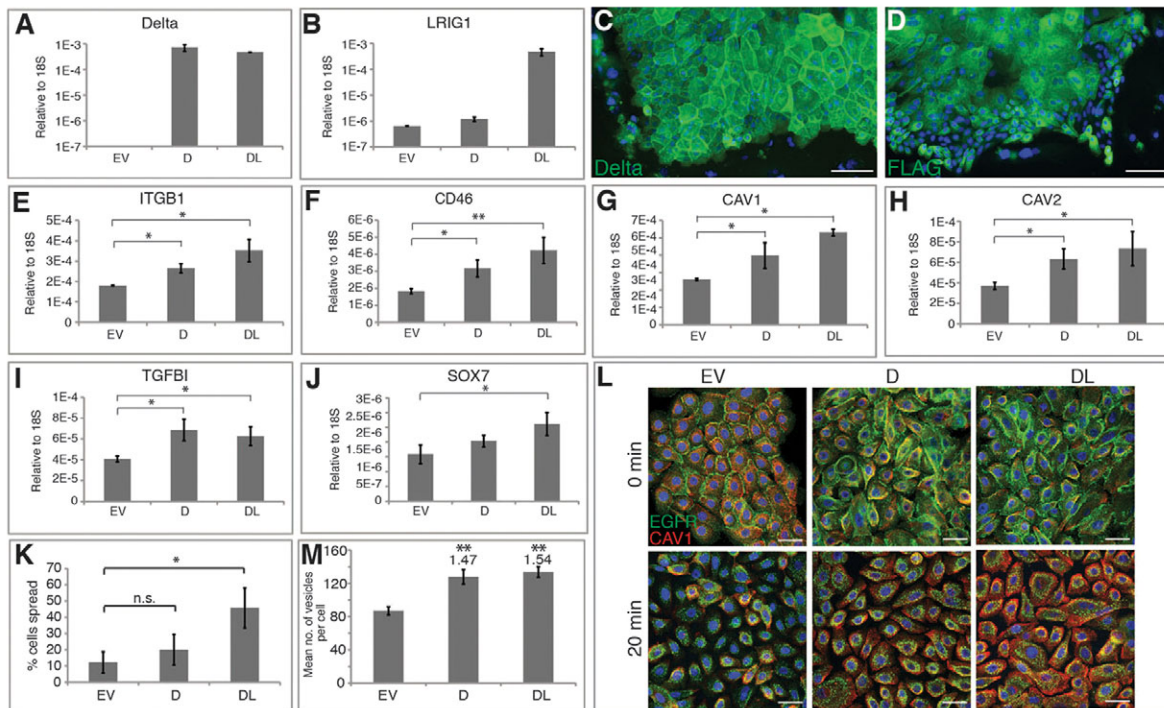


Fig. 5. Stem cell markers are not independently regulated. (A,B) QPCR expression data for zebrafish *delta* (A) and *LRIG1* (B) in keratinocytes retrovirally infected with *delta* alone (D) or together with *LRIG1* (DL); control cells were infected with empty vector (EV). (C,D) Immunostaining for zebrafish Delta (C, green) and FLAG (D, green) with DAPI counterstain (blue). (E-J) QPCR expression data for six genes identified as upregulated in D+ cells. $n=4$ experiments. * $P<0.05$; ** $P<0.01$. (K) Quantitation of percentage spread cells after adhesion to type I collagen for 30 minutes. $n=3$ experiments. * $P=0.0418$ for DL; n.s.: not significant. (L) Immunostaining for EGFR (green) and CAV1 (red) with DAPI nuclear counterstain (blue). Cells were serum starved (0 minute) or treated with EGF for 20 minutes. (M) Quantitation of vesicles in L. $n=3$ experiments. Values above columns indicate fold-change compared with empty vector (EV) control. ** $P=0.00229$ for D, ** $P=0.00828$ for DL. Data are mean \pm s.e.m. Scale bars: 50 μ m.

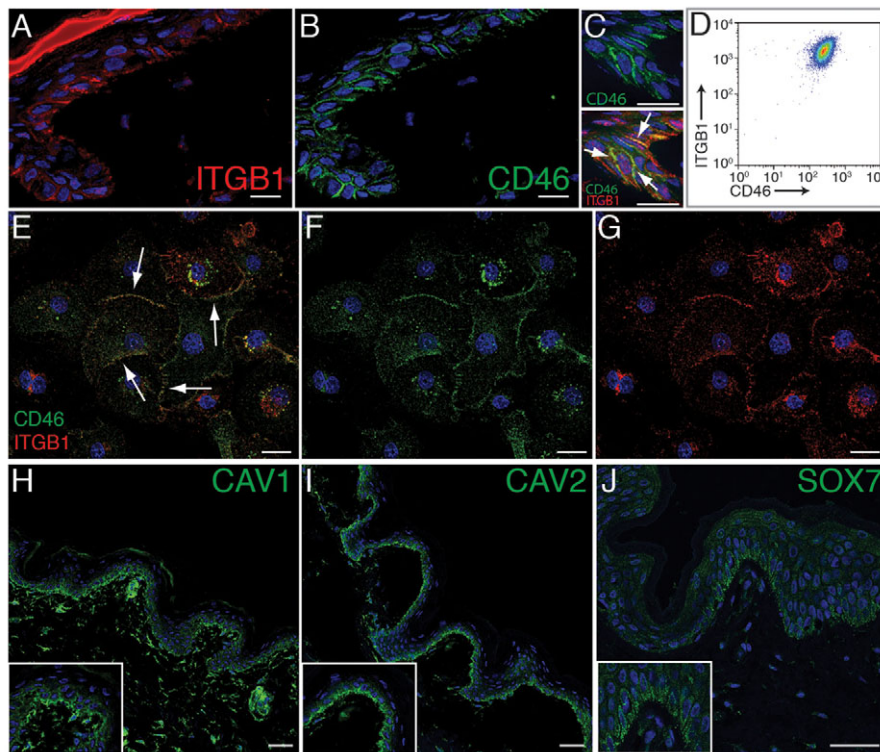


Fig. 6. Epidermal expression of CD46, CAV1, CAV2 and SOX7. (A-C) Immunofluorescence staining of CD46 (green) and ITGB1 (red) in human abdomen skin. The same field is shown in A and B. (C) High magnification view of the epidermal basal layer showing CD46 (green) only (top) or double labelling for ITGB1 (red) (bottom). Arrows indicate co-expression of CD46 and ITGB1 at cell-cell junctions. (D) Flow cytometry dot plot showing co-expression of CD46 and ITGB1 in cultured primary human keratinocytes gated on the basis of low forward and side scatter (undifferentiated cells). (E-G) Immunofluorescence staining of CD46 (green) and ITGB1 (red) in cultured primary human keratinocytes showing colocalisation at cell-cell junctions (arrows). (E) Merged of F and G. (H-J) Immunofluorescence staining for CAV1 (H), CAV2 (I) and SOX7 (J) in adult human abdomen skin showing positive staining in the basal epidermal layer (green). Insets show higher magnification views of basal layer staining. Cells and sections were counterstained with DAPI (blue). Scale bars: 50 μ m in A-C; 10 μ m in E-G; 100 μ m in H-J.

CD46 is a novel marker that enriches for epidermal stem cells

A number of genes that were upregulated in the D+ cluster have not been previously implicated as potential epidermal stem cell markers. CD46 (Fig. 6A-G), CAV1 (Fig. 6H), CAV2 (Fig. 6I), SOX7 (Fig. 6J) and CKAP2 (<http://www.proteinatlas.org/ENSG00000136108/normal/skin>) all showed strong expression in the basal layer of human epidermis and were downregulated during terminal differentiation.

To obtain experimental evidence that we could indeed identify new markers that enrich for human epidermal stem cells, we explored the expression and function of CD46 (which is also known as membrane co-factor protein). CD46 was one of the most highly upregulated genes (8.07-fold) in the D+ cluster. CD46 is a type I transmembrane glycoprotein that was originally discovered as a complement regulatory protein (Seya and Atkinson, 1989; Liszewski et al., 1991). CD46 regulates T-cell cytokine production (Cardone et al., 2010) and is a cell surface receptor for several human pathogens (Cattaneo, 2004).

Of particular relevance to the epidermis, CD46 colocalises with β 1 integrins (McLaughlin et al., 2003) and, like β 1 integrins, binds tetraspans such as CD9 (Rubinstein et al., 1996; Lozahic et al., 2000). Antibodies to β 1 integrins or CD9 can inhibit suspension-induced terminal differentiation of human keratinocytes (Jones et al., 1996). In human epidermis, CD46, like β 1 integrins, was expressed in the basal layer and downregulated in the suprabasal, differentiating cell layers (Fig. 6A,B) (Jones et al., 1995). There was extensive colocalisation of CD46 with β 1 integrins at cell-cell borders in the epidermis (Fig. 6C, arrows) and in cultured human epidermal keratinocytes (Fig. 6E-G). When differentiated, suprabasal cells were gated out on the basis of high forward and side scatter, flow cytometry confirmed co-expression of CD46 and β 1 integrins on the surface of cultured basal keratinocytes (Fig. 6D).

To determine whether keratinocytes expressing high levels of CD46 also expressed high levels of Dll1 and β 1 integrin, basal cells were sorted according to whether they expressed high or low levels of CD46 (CD46^{high} or CD46^{low}, respectively) or were CD46-negative (CD46^{neg}) (Fig. 7A). QPCR established that the cells with the highest level of CD46 (Fig. 7B) also had the highest levels of *DLL1* and *ITGB1* (Fig. 7C,D). CD46^{high} cells showed a higher rate of proliferation than CD46^{low} cells, whereas CD46^{neg} cells failed to proliferate, suggesting that they were committed to terminal differentiation (Fig. 7E). CD46^{high} cells had a considerably greater colony forming efficiency than CD46^{low} and CD46^{neg} cells (Fig. 7F).

In addition to their capacity for extensive self-renewal, a key feature of human epidermal stem cells is their high ECM adhesiveness (Adams and Watt, 1989; Watt, 2002). According to our microarray data, adhesion and proliferation are important features of D+ cluster cells (Fig. 4C). To assay the adhesiveness of cells expressing different levels of CD46, flow-sorted populations were allowed to adhere and spread on collagen I for 30 minutes. Of the cells that did adhere, the proportion of spread cells was similar in the CD46^{high} and CD46^{low} populations. However, the number of CD46^{high} cells that adhered was ~50% greater than that of CD46^{low} cells and most CD46^{neg} cells failed to adhere at all (Fig. 7H-K).

IPA analysis (Fig. 7G) provided independent confirmation of a positive relationship between the expression of CD46 and ITGB1, the tetraspans CD9, CD81, CD82 and CD151, and caveolins 1 and 2. We conclude that, as predicted from single-cell global gene expression profiling, CD46 is a new marker of human epidermal stem cells that enriches for adhesive and clonogenic cells.

CD46 expression is required for epidermal stem cell renewal and β 1 integrin-mediated adhesion

To test whether CD46 is required to maintain the adhesive and proliferative properties of human epidermal stem cells we

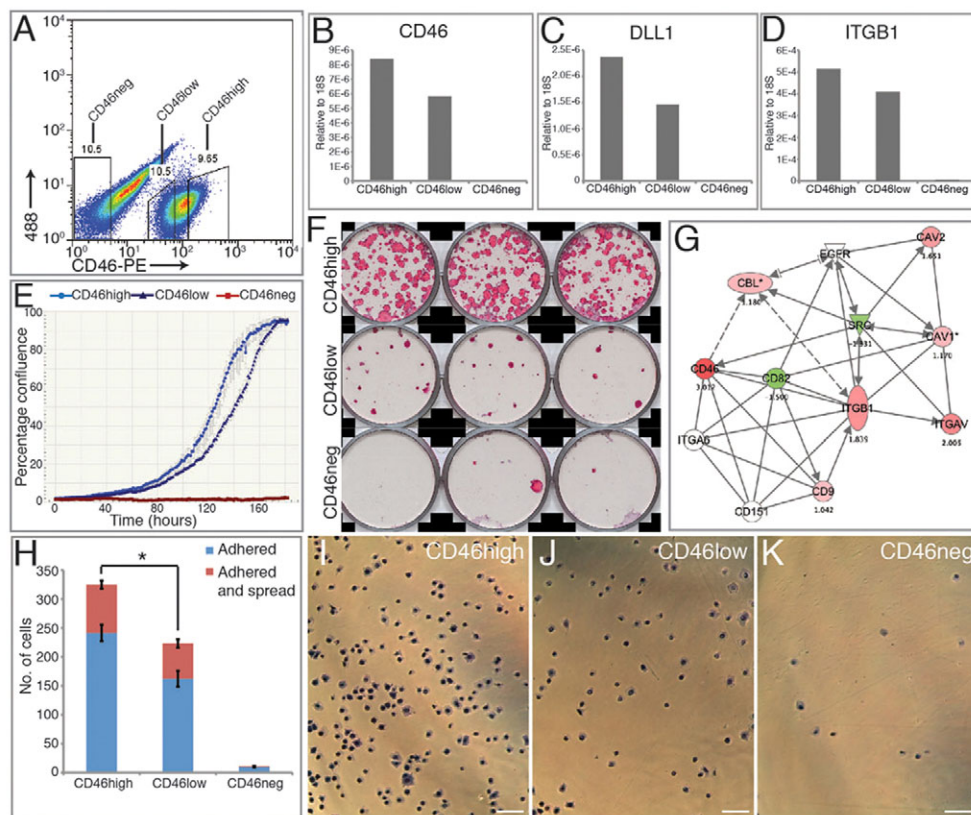


Fig. 7. High cell surface levels of CD46 enrich for epidermal stem cells. (A) Flow cytometry dot plot of undifferentiated keratinocytes (low forward and side scatter) showing gates for isolating cells with high (CD46high), low (CD46low) and no (CD46neg) surface levels of CD46. (B–D) QPCR quantitation of mRNA levels of *CD46* (B), *DLL1* (C) and *ITGB1* (D) in one experiment, representative of three independent experiments, showing enrichment of stem cell marker genes in the CD46high population. (E) Growth curves obtained in an IncuCyte system. (F) Clonal growth assays, representative of four independent experiments. (G) Ingenuity network analysis showing relationship between CD46 and genes that regulate $\beta 1$ integrin-mediated adhesion and EGFR signalling. Green represents downregulation and red represents upregulation in D+ compared with D– cells (\log_2 -fold change values are shown below coloured nodes). (H) Quantitation of adherent and spread cells following plating on type I collagen for 30 minutes. Data are mean \pm s.e.m., $n=3$. * $P=0.0182$. (I–K) Representative images of adherent and spread cells. Scale bars: 50 μ m.

performed transient siRNA-mediated knockdown of CD46. The expression level of *CD46* mRNA was reduced by 92.8% using a pool of four different siRNAs (Fig. 8A). To control for off-target effects, each siRNA was also introduced individually into keratinocytes, resulting in a knockdown efficiency of between 55.7% and 93.2% (Fig. 8A; data not shown).

Knockdown of CD46 resulted in a concomitant decrease in *ITGB1* mRNA (Fig. 8B) and in the level of $\beta 1$ integrin on the cell surface (Fig. 8C,D). In addition, there was a reduction in the expression of the tetraspans CD9 and CD82, as well as of CBL, a CD46-induced adaptor protein that regulates cell signalling (Fig. 8E–G). The biological significance of these changes remains to be determined, but it is notable that CBL has previously been shown to be induced by CD46 (Ota and Samelson, 1997; Murphy et al., 1998). Although overexpression of *DLL1* led to an increase in CD46 (Fig. 5F), knockdown of CD46 did not lead to a reduction in *DLL1* (Fig. 8H).

siRNA-mediated knockdown of CD46 resulted in a marked reduction in keratinocyte adhesion and spreading on type I collagen (Fig. 8I) and a marked decrease in keratinocyte growth rate (Fig. 8J). Control keratinocytes grew to confluence by 7 days, whereas siRNA-treated cells failed to grow even when monitored for 10 days (Fig. 8J).

We conclude that CD46, identified by single-cell global gene expression profiling, is not only a new marker of human epidermal stem cells, but also plays a role in stem cell function, as it is required for cells to adhere and self-renew.

DISCUSSION

There is growing evidence that stem cell fate control involves both deterministic and stochastic processes. Complex regulatory networks define stable, interconvertible ‘attractor’ states and stochastic fluctuations in gene expression (transcriptional noise) drive transitions between states (MacArthur et al., 2008; Enver et al., 2009; Pina et al., 2012). Population-based studies, in which cells are judged homogeneous on the basis of flow cytometry profiles, lack the resolution to reveal heterogeneity resulting from different attractor states and to uncover its functional significance (Kalmar et al., 2009).

By adopting a single-cell approach, we found that *DLL1* is a key discriminator between two populations of undifferentiated basal keratinocytes that differ in adhesion and proliferation. The two clusters have distinct transcriptional profiles, indicating that intercellular differences in gene expression cannot be attributed solely to random stochastic fluctuations. As a validation of our approach, we identified CD46 as a novel cell surface marker of

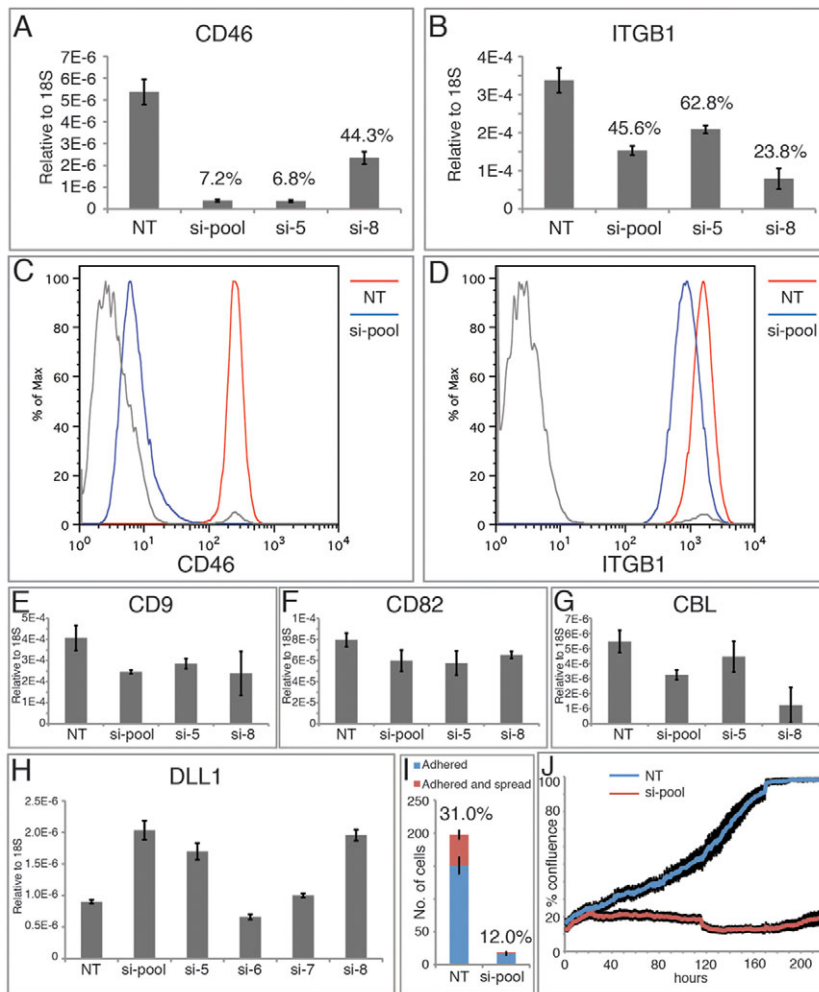


Fig. 8. siRNA-mediated knockdown of CD46 decreases proliferation and $\beta 1$ integrin-mediated adhesion. (A,B) QPCR quantitation of *CD46* (A) and *ITGB1* (B) mRNA levels after siRNA-mediated knockdown of CD46. $n=4$. NT, non-targeting control; si-pool, pool of four different siRNAs against *CD46*; si-5 and si-8, two individual siRNAs against *CD46*. Values shown above each column indicate percentage expression that remains 72 hours post-treatment. (C,D) Cell surface levels of CD46 (C) and ITGB1 (D) determined by flow cytometry of undifferentiated cells (low forward and side scatter). Grey lines, negative control. (E-H) QPCR quantitation of *CD9* (E), *CD82* (F), *CBL* (G) and *DLL1* (H) mRNA levels 72 hours post-*CD46* knockdown. $n=4$. (I) Quantitation of adherent and spread cells following plating on type I collagen for 30 minutes. $n=3$. (J) Effect of *CD46* knockdown on growth curves. Data are mean \pm s.e.m.

human epidermal stem cells. These findings underscore the utility of high-resolution strategies to search for stem cell markers and explore stem cell function. Cellular heterogeneity within the proliferative compartment of mouse tail IFE has recently been demonstrated (Mascré et al., 2012) and it will be interesting to discover whether or not these cells differ in expression of CD46 or in any of the other markers upregulated in the human D⁺ cluster.

Although the two states defined by DLL1 expression may be intrinsic, we speculate that they are reinforced by virtue of their influence on how cells interact with the environment, for example through ECM adhesion and caveolin-mediated endocytosis. This would be consistent with recent experiments in which we discovered a network of genetic interactions involving distinct chromatin modifiers that impact distinct but functionally related gene sets, including integrin ECM receptors (Mulder et al., 2012).

IPA analysis predicted that cells in the D⁺ cluster would exhibit altered integrin-mediated adhesion and increased caveolin-mediated endocytosis, and this was confirmed by overexpressing *delta* and *LRIG1*. *DLL1* overexpression resulted in increased expression of $\beta 1$ integrins and genes associated with receptor tyrosine kinase signalling and endocytosis. The marker that discriminated best between the two clusters was syntenin, which not only interacts with the cytoplasmic domain of DLL1, but also with $\beta 1$ integrins and MCSP, two further stem cell markers (Beekman and Coffey, 2008). There are clear parallels with stem cells in the *Drosophila* intestine,

where Delta is also a stem cell marker (Ohlstein and Spradling, 2007).

In addition to CD46, CAV1 and CAV2 were upregulated in the D⁺ cluster and shown to be expressed in the epidermal basal layer. Overexpression of DLL1 resulted in increased caveolin-dependent endocytosis of EGFR in EGF-stimulated cells. These findings are particularly interesting in the light of other studies suggesting a link between caveolins and stem cells. CAV1 expression regulates the size of the stem cell compartment in adult mouse mammary gland and intestine (Mercier et al., 2009), and *Cav1*^{-/-} mice exhibit hypersensitivity to carcinogen-induced epidermal tumours (Capozza et al., 2003). Caveolin lipid rafts in the plasma membrane facilitate crosstalk between different signalling receptors (Razani et al., 2002) and are involved in the coordination and coupling of $\beta 1$ integrin, Notch1 and receptor tyrosine kinase signalling pathways (Campos et al., 2006). The caveolin-scaffolding domain itself is a docking site for signalling components of proliferative and pro-survival pathways (Mercier et al., 2009). All this suggests that the upregulation of caveolins in epidermal stem cells might play a role in regulating proliferative signalling pathways.

One striking observation was that overexpression of *delta* and *LRIG1* resulted in increased expression of *ITGB1* and other genes in the D⁺ cluster. Although the underlying mechanism remains to be explored, it is interesting to consider that it might reflect an altered sensitivity to microenvironmental cues. For example, there is evidence that cell-cell adhesion positively regulates expression of

SOX7, one of the D+ genes (Bauwens et al., 2011), and we have previously demonstrated that *DLL1* promotes intercellular adhesion (Lowell et al., 2000; Lowell and Watt, 2001; Estrach et al., 2007). Although CD46 knockdown did not reduce *DLL1* expression, it did result in reduced $\beta 1$ integrin mRNA and protein levels. CD46high stem cells had elevated levels of *DLL1* and $\beta 1$ integrins and exhibited enhanced adhesion and proliferative potential. Adhesiveness to the epidermal basement membrane could affect the response to other extracellular niche signals, including growth factors. Thus, the intrinsic and extrinsic regulators of epidermal stem cells are not independent, but tightly interconnected.

Acknowledgements

We thank Emma Heath, Elizabeth Jane MacRae, Peter Humphreys and Emily Clemente for technical support.

Funding

This work was funded by the Medical Research Council, Wellcome Trust, Cancer Research UK and EU FP7 programme TUMIC. D.W.M.T. received a National Science Scholarship (PhD) from the Agency for Science, Technology and Research, Singapore (A*STAR). Deposited in PMC for immediate release.

Competing interests statement

M.W.B.T. is an employee of Celgene Research (Spain), part of Celgene.

Supplementary material

Supplementary material available online at <http://dev.biologists.org/lookup/suppl/doi:10.1242/dev.087551/-DC1>

References

- Adams, J. C. and Watt, F. M. (1989). Fibronectin inhibits the terminal differentiation of human keratinocytes. *Nature* **340**, 307-309.
- Barrandon, Y. and Green, H. (1987). Three clonal types of keratinocyte with different capacities for multiplication. *Proc. Natl. Acad. Sci. USA* **84**, 2302-2306.
- Bauwens, C. L., Song, H., Thavandiran, N., Ungrin, M., Massé, S., Nanthakumar, K., Seguin, C. and Zandstra, P. W. (2011). Geometric control of cardiomyogenic induction in human pluripotent stem cells. *Tissue Eng. Part A* **17**, 1901-1909.
- Beekman, J. M. and Coffey, P. J. (2008). The ins and outs of syntenin, a multifunctional intracellular adaptor protein. *J. Cell Sci.* **121**, 1349-1355.
- Campos, L. S., Decker, L., Taylor, V. and Skarnes, W. (2006). Notch, epidermal growth factor receptor, and beta1-integrin pathways are coordinated in neural stem cells. *J. Biol. Chem.* **281**, 5300-5309.
- Capozza, F., Williams, T. M., Schubert, W., McClain, S., Bouzahzah, B., Sotgia, F. and Lisanti, M. P. (2003). Absence of caveolin-1 sensitizes mouse skin to carcinogen-induced epidermal hyperplasia and tumor formation. *Am. J. Pathol.* **162**, 2029-2039.
- Cardone, J., Le Fric, G., Vantourout, P., Roberts, A., Fuchs, A., Jackson, I., Suddason, T., Lord, G., Atkinson, J. P., Cope, A. et al. (2010). Complement regulator CD46 temporally regulates cytokine production by conventional and unconventional T cells. *Nat. Immunol.* **11**, 862-871.
- Cattaneo, R. (2004). Four viruses, two bacteria, and one receptor: membrane cofactor protein (CD46) as pathogens' magnet. *J. Virol.* **78**, 4385-4388.
- Chang, H. H., Hemberg, M., Barahona, M., Ingber, D. E. and Huang, S. (2008). Transcriptome-wide noise controls lineage choice in mammalian progenitor cells. *Nature* **453**, 544-547.
- de Hoon, M. J., Imoto, S., Nolan, J. and Miyano, S. (2004). Open source clustering software. *Bioinformatics* **20**, 1453-1454.
- De Luca, M., Pellegrini, G. and Green, H. (2006). Regeneration of squamous epithelia from stem cells of cultured grafts. *Regen. Med.* **1**, 45-57.
- Enver, T., Pera, M., Peterson, C. and Andrews, P. W. (2009). Stem cell states, fates, and the rules of attraction. *Cell Stem Cell* **4**, 387-397.
- Estrach, S., Legg, J. and Watt, F. M. (2007). Syntenin mediates Delta1-induced cohesiveness of epidermal stem cells in culture. *J. Cell Sci.* **120**, 2944-2952.
- Frye, M., Gardner, C., Li, E. R., Arnold, I. and Watt, F. M. (2003). Evidence that Myc activation depletes the epidermal stem cell compartment by modulating adhesive interactions with the local microenvironment. *Development* **130**, 2793-2808.
- Green, H. (2008). The birth of therapy with cultured cells. *BioEssays* **30**, 897-903.
- Gur, G., Rubin, C., Katz, M., Amit, I., Citri, A., Nilsson, J., Amarglio, N., Henriksson, R., Rechavi, G., Hedman, H. et al. (2004). LRIG1 restricts growth factor signaling by enhancing receptor ubiquitylation and degradation. *EMBO J.* **23**, 3270-3281.
- Jaks, V., Kasper, M. and Toftgård, R. (2010). The hair follicle—a stem cell zoo. *Exp. Cell Res.* **316**, 1422-1428.
- Janes, S. M., Ofstad, T. A., Campbell, D. H., Watt, F. M. and Prowse, D. M. (2004). Transient activation of FOXP1 in keratinocytes induces a transcriptional programme that promotes terminal differentiation: contrasting roles of FOXP1 and Akt. *J. Cell Sci.* **117**, 4157-4168.
- Jensen, K. B. and Watt, F. M. (2006). Single-cell expression profiling of human epidermal stem and transit-amplifying cells: Lrig1 is a regulator of stem cell quiescence. *Proc. Natl. Acad. Sci. USA* **103**, 11958-11963.
- Jensen, U. B., Lowell, S. and Watt, F. M. (1999). The spatial relationship between stem cells and their progeny in the basal layer of human epidermis: a new view based on whole-mount labelling and lineage analysis. *Development* **126**, 2409-2418.
- Jones, P. H. and Watt, F. M. (1993). Separation of human epidermal stem cells from transit amplifying cells on the basis of differences in integrin function and expression. *Cell* **73**, 713-724.
- Jones, P. H., Harper, S. and Watt, F. M. (1995). Stem cell patterning and fate in human epidermis. *Cell* **80**, 83-93.
- Jones, P. H., Bishop, L. A. and Watt, F. M. (1996). Functional significance of CD9 association with beta 1 integrins in human epidermal keratinocytes. *Cell Adhes. Commun.* **4**, 297-305.
- Kalmar, T., Lim, C., Hayward, P., Muñoz-Descalzo, S., Nichols, J., Garcia-Ojalvo, J. and Martinez Arias, A. (2009). Regulated fluctuations in nanog expression mediate cell fate decisions in embryonic stem cells. *PLoS Biol.* **7**, e1000149.
- Kurimoto, K., Yabuta, Y., Ohinata, Y., Ono, Y., Uno, K. D., Yamada, R. G., Ueda, H. R. and Saitou, M. (2006). An improved single-cell cDNA amplification method for efficient high-density oligonucleotide microarray analysis. *Nucleic Acids Res.* **34**, e42.
- Kurimoto, K., Yabuta, Y., Ohinata, Y. and Saitou, M. (2007). Global single-cell cDNA amplification to provide a template for representative high-density oligonucleotide microarray analysis. *Nat. Protoc.* **2**, 739-752.
- Le Borgne, R. (2006). Regulation of Notch signalling by endocytosis and endosomal sorting. *Curr. Opin. Cell Biol.* **18**, 213-222.
- Legg, J., Jensen, U. B., Broad, S., Leigh, I. and Watt, F. M. (2003). Role of melanoma chondroitin sulphate proteoglycan in patterning stem cells in human interfollicular epidermis. *Development* **130**, 6049-6063.
- Liszewski, M. K., Post, T. W. and Atkinson, J. P. (1991). Membrane cofactor protein (MCP or CD46): newest member of the regulators of complement activation gene cluster. *Annu. Rev. Immunol.* **9**, 431-455.
- Lowell, S. and Watt, F. M. (2001). Delta regulates keratinocyte spreading and motility independently of differentiation. *Mech. Dev.* **107**, 133-140.
- Lowell, S., Jones, P., Le Roux, I., Dunne, J. and Watt, F. M. (2000). Stimulation of human epidermal differentiation by delta-notch signalling at the boundaries of stem-cell clusters. *Curr. Biol.* **10**, 491-500.
- Lozahic, S., Christiansen, D., Manié, S., Gerlier, D., Billard, M., Boucheix, C. and Rubinstein, E. (2000). CD46 (membrane cofactor protein) associates with multiple beta1 integrins and tetraspans. *Eur. J. Immunol.* **30**, 900-907.
- MacArthur, B. D., Please, C. P. and Oreffo, R. O. (2008). Stochasticity and the molecular mechanisms of induced pluripotency. *PLoS ONE* **3**, e3086.
- Mascré, G., Dekoninck, S., Drogat, B., Youssef, K. K., Brohé, S., Sotiropoulou, P. A., Simons, B. D. and Blanpain, C. (2012). Distinct contribution of stem and progenitor cells to epidermal maintenance. *Nature* **489**, 257-262.
- McLaughlin, B. J., Fan, W., Zheng, J. J., Cai, H., Del Priore, L. V., Bora, N. S. and Kaplan, H. J. (2003). Novel role for a complement regulatory protein (CD46) in retinal pigment epithelial adhesion. *Invest. Ophthalmol. Vis. Sci.* **44**, 3669-3674.
- Mercier, I., Jasmin, J. F., Pavlides, S., Minetti, C., Flomenberg, N., Pestell, R. G., Frank, P. G., Sotgia, F. and Lisanti, M. P. (2009). Clinical and translational implications of the caveolin gene family: lessons from mouse models and human genetic disorders. *Lab. Invest.* **89**, 614-623.
- Mulder, K. W., Wang, X., Escru, C., Ito, Y., Schwarz, R. F., Gillis, J., Sirokmány, G., Donati, G., Uribe-Lewis, S., Pavlidis, P. et al. (2012). Diverse epigenetic strategies interact to control epidermal differentiation. *Nat. Cell Biol.* **14**, 753-763.
- Murphy, M. A., Schnell, R. G., Venter, D. J., Barnett, L., Bertonecello, I., Thien, C. B., Langdon, W. Y. and Bowtell, D. D. (1998). Tissue hyperplasia and enhanced T-cell signalling via ZAP-70 in c-Cbl-deficient mice. *Mol. Cell Biol.* **18**, 4872-4882.
- Nichols, J. T., Miyamoto, A. and Weinmaster, G. (2007). Notch signaling – constantly on the move. *Traffic* **8**, 959-969.
- Oates, A. C. (2011). What's all the noise about developmental stochasticity? *Development* **138**, 601-607.
- Ohlstein, B. and Spradling, A. (2007). Multipotent Drosophila intestinal stem cells specify daughter cell fates by differential notch signaling. *Science* **315**, 988-992.
- Osawa, M., Egawa, G., Mak, S. S., Moriyama, M., Freter, R., Yonetani, S., Beermann, F. and Nishikawa, S. (2005). Molecular characterization of melanocyte stem cells in their niche. *Development* **132**, 5589-5599.
- Ota, Y. and Samelson, L. E. (1997). The product of the proto-oncogene c-cbl: a negative regulator of the Syk tyrosine kinase. *Science* **276**, 418-420.

- Pina, C., Fugazza, C., Tipping, A. J., Brown, J., Soneji, S., Teles, J., Peterson, C. and Enver, T.** (2012). Inferring rules of lineage commitment in haematopoiesis. *Nat. Cell Biol.* **14**, 287-294.
- Raj, A., van den Bogaard, P., Rifkin, S. A., van Oudenaarden, A. and Tyagi, S.** (2008). Imaging individual mRNA molecules using multiple singly labeled probes. *Nat. Methods* **5**, 877-879.
- Razani, B., Woodman, S. E. and Lisanti, M. P.** (2002). Caveolae: from cell biology to animal physiology. *Pharmacol. Rev.* **54**, 431-467.
- Rubinstein, E., Le Naour, F., Lagaudrière-Gesbert, C., Billard, M., Conjeaud, H. and Boucheix, C.** (1996). CD9, CD63, CD81, and CD82 are components of a surface tetraspan network connected to HLA-DR and VLA integrins. *Eur. J. Immunol.* **26**, 2657-2665.
- Segatto, O., Anastasi, S. and Alemà, S.** (2011). Regulation of epidermal growth factor receptor signalling by inducible feedback inhibitors. *J. Cell Sci.* **124**, 1785-1793.
- Seya, T. and Atkinson, J. P.** (1989). Functional properties of membrane cofactor protein of complement. *Biochem. J.* **264**, 581-588.
- Storey, J. D. and Tibshirani, R.** (2003). Statistical significance for genome-wide studies. *Proc. Natl. Acad. Sci. USA* **100**, 9440-9445.
- Wang, W. and Struhl, G.** (2004). Drosophila Epsin mediates a select endocytic pathway that DSL ligands must enter to activate Notch. *Development* **131**, 5367-5380.
- Watt, F. M.** (2002). Role of integrins in regulating epidermal adhesion, growth and differentiation. *EMBO J.* **21**, 3919-3926.
- Watt, F. M., Broad, S. and Prowse, D. M.** (2006) Cultivation and retroviral infection of human epidermal keratinocytes. In *Cell Biology: A Laboratory Handbook*, Vol. 1, 3rd edn (ed. J. E. Celis), pp. 133-138. London: Elsevier Academic Press.
- Zhu, A. J., Haase, I. and Watt, F. M.** (1999). Signaling via beta1 integrins and mitogen-activated protein kinase determines human epidermal stem cell fate in vitro. *Proc. Natl. Acad. Sci. USA* **96**, 6728-6733.